IEEE Photonics Journal
An IEEE Photonics Society Publication

Open Access

# 2-D Grating Couplers for Vertical Fiber Coupling in Two Polarizations

Volume 11, Number 4, August 2019

**Tatsuhiko Watanabe**, *Member, IEEE*
**Yuriy Fedoryshyn**
**Juerg Leuthold**, *Fellow, IEEE*

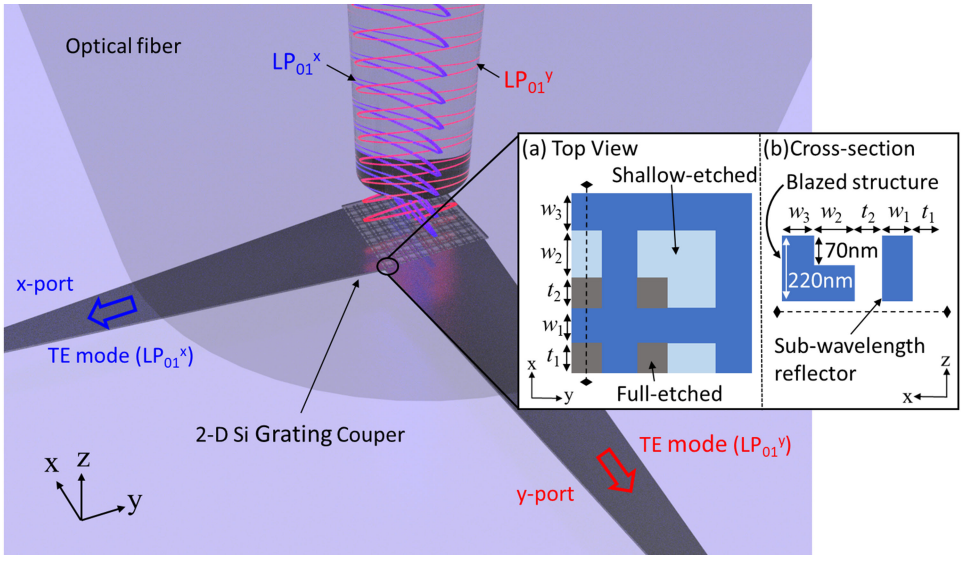


DOI: 10.1109/JPHOT.2019.2926823

# 2-D Grating Couplers for Vertical Fiber Coupling in Two Polarizations

**Tatsuhiko Watanabe, *Member, IEEE*, Yuriy Fedoryshyn, and Juerg Leuthold, *Fellow, IEEE***

Institute of Electromagnetics Fields, Zurich 8092, Switzerland

*DOI:10.1109/JPHOT.2019.2926823*


Manuscript received May 8, 2019; revised June 27, 2019; accepted June 29, 2019. Date of publication June 13, 2019; date of current version July 22, 2019. This work was supported by "ETH Zurich Postdoctoral Fellowship" from the European Union's Seventh Framework Programme for research, technological development, and demonstration under Grant 608881. Corresponding author: Tatsuhiko Watanabe (e-mail: tatsuhiko.watanabe@ief.ee.ethz.ch).

**Abstract:** We demonstrate highly efficient couplers in a two-dimensional grating configuration for a vertical fiber-coupling fabricated in the silicon-on-insulator platform. A combination of sub-wavelength reflectors and blazed gratings enables both high coupling efficiency and vertical grating coupling. We experimentally achieve coupling efficiencies of $-2.6$ dB at 1544 nm and $-3.4$ dB at 1536 nm for x- and y-polarized LP01 modes, respectively. The experimental results are in good agreement with the simulated $-2.4$ dB coupling efficiency for both polarizations at a wavelength of 1550 nm. Simulated and measured crosstalk between two polarizations were $-19$ dB and $<-16$ dB, respectively.

**Index Terms:** Grating coupler, polarization diversity, silicon photonics.

## 1. Introduction

Silicon-on-insulator (SOI) has become an established platform for photonics. Consequently, efficient fiber-to-chip coupling is crucial for practical applications. Meanwhile there are many solutions that offer efficient coupling for a given linear polarization light. However, in practical applications such as sensing and coherent communications an efficient coupling of both polarizations is needed. Thus, ideally, such couplers should offer efficient coupling for both polarizations with a high extinction ratio to cross-polarizations. Furthermore, the ideal coupler should feature fabrication and alignment tolerance with a simple vertical coupling scheme.

Single polarization grating couplers with experimental coupling efficiencies of higher than 80% [1]–[3] and 70% [4] in tilted and vertical fiber schemes, respectively, have already been demonstrated on a standard SOI platform. Simulations even predict coupling efficiencies approaching 90% [4], [5] and more [3], [6]. These achievements are in part due to the introduction of apodization schemes [7]–[9], blazed gratings [10] and an improvement of the fabrication technologies [11]. More recently the interest has shifted towards 2-dimensional (2-D) grating couplers which comprise two orthogonal 1-D grating couplers superimposed on each other. The 2-D grating couplers couple the x- and y-polarized $LP_{01}$ modes of the input fiber onto two separate outputs. In this process both the x- and y-polarized $LP_{01}$ modes are then converted to TE modes of the silicon waveguide on the chip. The 2-D grating couplers thus also act as a polarization splitter. Ever since the first demonstration in 2003 [12], several attempts to realize highly efficient 2-D grating coupler on the SOI platform have been made. Subsequent studies have used novel techniques including photonic crystals

TABLE 1
Comparison of 2-D Grating Couplers

| Ref. | Year | Fiber angle | CE Sim. | CE Exp. | Wavelength | Metal mirror | Platform |
|---|---|---|---|---|---|---|---|
| [12] | 2003 | 0° | - | −7.0dB | 1550 | w/o | SOI |
| [15] | 2009 | 10° | - | −5.6dB | 1550 | w/o | SOI |
| [22] | 2010 | 0° | −4.0dB | −5.2dB | 1550 | w/o | SOI |
| [23] | 2010 | 0° | | -4.0dB | 1550 | w/o | SOI |
| [16] | 2014 | 8° | - | −2.0dB | 1480 | w/o | Double SOI |
| [24] | 2014 | 0° | −4.0dB | −5.5dB | 1550 | w/o | SOI |
| [25] | 2015 | 0° | - | −4.8dB | 1550 | w/o | SOI |
| [17] | 2016 | 15° | −3.2dB | −3.7dB | 1550 | w/o | SOI |
| [18] | 2016 | 6° | −3.2dB | −3.3dB | 1310 | w/o | SOI |
| [13] | 2017 | 10° | −4.0dB | - | 1550 | w/o | SOI |
| | | | −1.7dB | - | 1550 | w/ | SOI |
| [14] | 2017 | 12° | −1.4dB | −1.8dB | 1550 | w/ | Si on BCB |
| This work | 2019 | 0° | −2.4dB | −2.6dB | 1550 | w/o | SOI |

and backside metal mirrors [13]–[18]. In those works, however, the grating couplers have been designed to couple fibers with a certain angle in order to suppress back-reflections. In some cases, e.g., when fiber arrays and multi-core fibers (MCF) are used [19]–[21] an angular alignment of the coupler not only costs much more space but also forces the access waveguides to be arranged in one direction – which significantly limits the integration density. For these reasons, 2-D grating couplers with perfect vertical coupling have been introduced [22]–[25]. A summary on the polarization multiplexed couplers with the coupling efficiencies is given in Table 1. As shown in Table 1, our 2-D grating coupler shows a significant improvement on the achievable coupling efficiency (CE) for perfect vertical coupling (fiber angle $= 0°$). Even compared with angled coupling schemes, it can outperform others fabricated on a standard SOI without a bottom-side metal mirror.

In this paper, we introduce highly efficient, polarization-splitting 2-D grating couplers, which provide a perfect vertical coupling to a single mode fiber (SMF) by utilizing a blazed sub-wavelength structure. We fabricated the 2-D grating on a standard silicon-on-insulator (SOI) platform and measured coupling losses of 2.6 dB and 3.4 dB for x- and y-polarizations, respectively, while simulations predict coupling efficiencies of 58% for each polarizations. Finally, we investigate the fabrication tolerances and derive its impact on the center peak shift.

Such a tilt-free grating coupler makes it easier to align fibers and offers more degree of freedoms to integrate grating couplers on a very small surface. Additionally, the 2-D grating coupler can be achieved using a standard SOI platform relying on a two-step etching process without introducing intricate fabrication procedures such as a metal mirror installation. The work published in this paper, is based in part on a 1D grating coupler configuration previously introduced in Ref. [4].

## 2. Concepts and Optimization

Figure 1 shows a concept of the 2-D grating coupler where $LP_{01}{}^{x}$ and $LP_{01}{}^{y}$ fiber modes are split into separated waveguides as TE polarized waveguide modes. (Remark: the two orthogonal $LP_{01}$ modes in the fiber are here called $LP_{01}{}^{x}$ and $LP_{01}{}^{y}$ modes for the sake of keeping nomenclature simple.) The fiber is vertically aligned to the chip surface without tilts. The high coupling efficiencies for the two polarizations are the results of an optimization of the 2-D grating coupler, the usage of an apodization and optimization of all parameters. The 2-D grating coupler comprises a superposition of two orthogonally aligned identical gratings. Fig. 1(a) shows the top view of a unit cell of the 2-D grating coupler. Each grating period consists of a combination of a blazed structure and a sub-wavelength structure as shown in Fig. 1(b) [4]. The blazed structure enhances a directionality

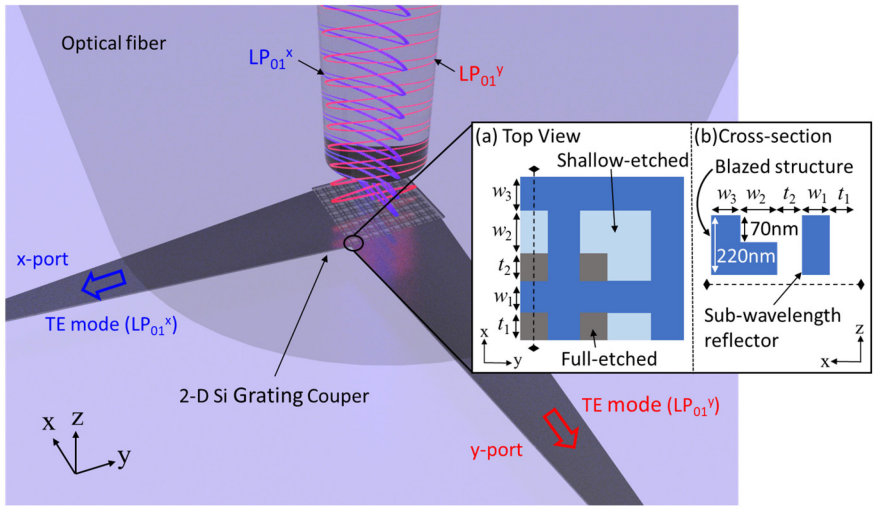


Fig. 1. Schematic view of the 2-dimensional grating coupler as a polarization splitter. The inset Figs. (a) and (b) represent structural details for one grating period viewed from top (xy-plane) and cross-section (xz-plane), respectively.

of the grating coupler [10] and the sub-wavelength structure provides an anti-reflection effect to suppress the back-reflections [26]. Thus, our grating can achieve perfect vertical coupling and a high coupling efficiency simultaneously without intricate structures such as a back-metal-mirror [27]–[30] and overlays [8], [31]. The superposition between etched and un-etched features of the two orthogonal gratings yields un-etched structures and the superposition between un-etched features remain un-etched whereas the superposition between etched features remain etched.

In order to achieve higher coupling efficiency we introduced an apodization scheme to the 2-D grating coupler. By introducing the apodization scheme we can tune a field profile of the diffracted light with some degrees of freedom. This benefits to improve a coupling efficiency of 2-D grating couplers in terms of two aspects: (i) increasing an overlap between fiber mode and diffracted light profiles; and (ii) having an identical alignment center axis for x- and y-polarization ports. In contrast, periodic grating couplers have a unique alignment center and a field profile due to the exponential decay of the diffracted light. First, we optimized the 2-D apodized grating coupler using a commercially available three-dimensional FDTD solver (by Lumerical). We assumed an SOI platform with a 220 nm-thick silicon layer and a 3 $\mu$m-thick buried oxide (BOX) layer. The depth of shallow etching areas was set to 70 nm. The refractive indices of Si and $SiO_2$ were 3.45 and 1.45, respectively. In the simulation, an x-polarized $LP_{01}$ mode was launched vertically to the 2-D grating coupler, and the transmittance into the x-port waveguide was used as a figure of merit and maximized through optimizations. The structural parameters for each grating period were optimized at a wavelength of 1550 nm by using a particle swarm algorithm [32].

The apodization of the grating was optimized as follows. We assumed that the 2-D grating coupler comprises two identical grating couplers superimposed, where each grating coupler has 20 periods with each period having 5 structural parameters (i.e., $t_1$, $t_2$, $w_1$, $w_2$, $w_3$). Thus, 100 ($20 \times 5$) parameters must be optimized in total. We expressed each structural parameter using a cubic spline interpolation with 5 knots sequence, so that the number of variables could be thinned down to 25 instead of 100 [4], [33]. Then, those knot values were optimized using the particle swarm algorithm. Here, we have set minimum feature sizes of trenches ($t_1$ and $t_2$) to $-40$ nm which corresponds to a resolution of our fabrication facility. Fig. 2(a) shows the optimized parameters. The knot sequences of the spline are marked by a diamond symbol. Fig. 2(b) shows the simulated spectra for the grating with the optimized data from Fig. 2(a). The straight blue line shows the coupling efficiency and the red line shows the crosstalk (XT) as induced by an opposite polarization. The coupling efficiency

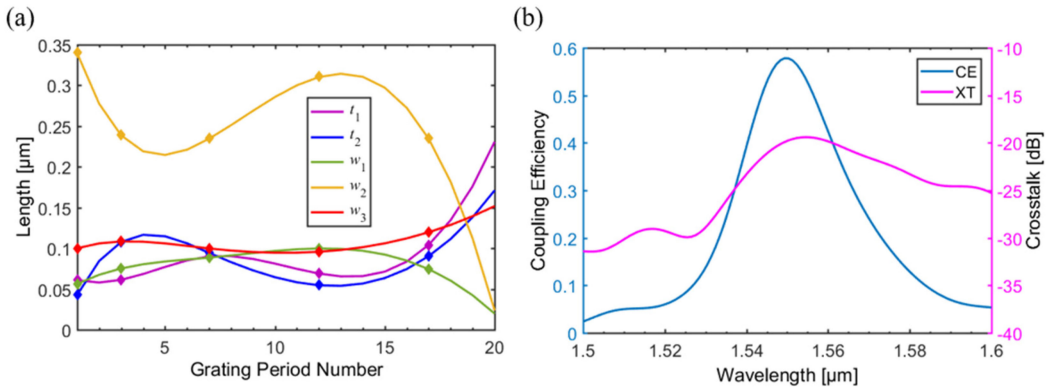


Fig. 2. Parameters of the optimized 2D grating and coupling efficiency. (a) Structural parameters optimized by the particle swarm algorithm with the coupling efficiency as the figure of merit. The diamonds are the spline knots optimized in simulation. They are used to fit a spline segments (separated by diamonds) to find the rest of the parameters. (b) Coupling efficiency and crosstalk of the optimized structure. The crosstalk is defined as the ratio of a power coupled into the opposite polarization port and the total input power.

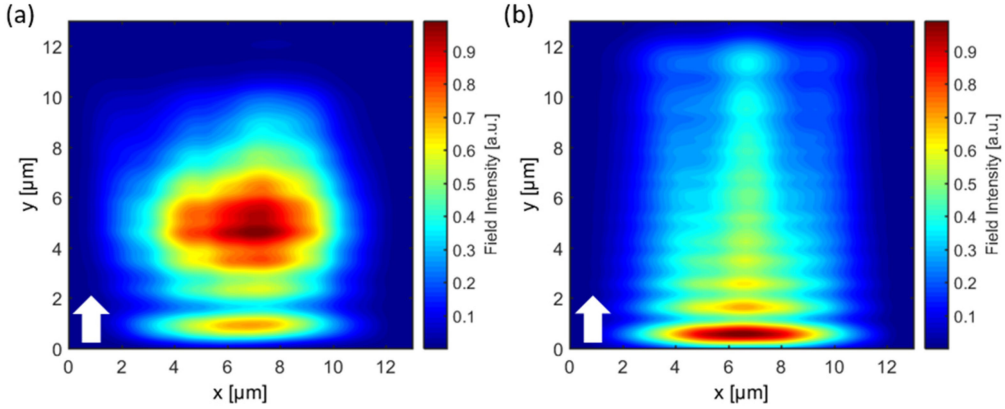


Fig. 3. Field intensity profiles radiated from (a) Apodized 2-D grating coupler and (b) Periodic 2-D grating coupler when the x-polarization port is excited (arrows show a direction of the excitation). The periodic structure was optimized at 1550 nm with the blazed and sub-wavelength structure ($t_1 = 77$ nm, $t_2 = 106$ nm, $w_1 = 77$ nm, $w_2 = 227$ nm, $w_3 = 105$ nm). Origins of x- and y-axes correspond to the starting point of gratings.

and the crosstalk were predicted to be $-2.4$ dB (58%) and $-19$ dB (1.2%) at the peak wavelength, respectively. Since the device has an axially symmetric structure and the fiber is positioned on the axis of symmetry, the transmission spectrum must be the same for both polarizations. The theoretical 3 dB bandwidth is relatively narrow (30 nm) as the apodization was optimized for the peak wavelength. We compare the field profiles diffracted by the apodized and periodic 2-D grating couplers in Fig. 3. In this simulation, the TE polarized waveguide mode is launched from the x-port waveguide along the y-axis, and the field profile is observed from the top of 2-D grating couplers. It can be seen in Fig. 3(a) that the field profile of the apodized grating coupler is similar to that of $LP_{01}$ modes. On the other hand, the periodic grating coupler has an exponential decaying field profile along the propagation direction. We confirmed that the field profile is successfully tuned by the apodization. We also can observe another peak of the field intensity in the vicinity of the origin of y axis in Fig. 3(a). This peak is primarily arising from an imperfection of the apodization on the first period of gratings, which is restricted by the minimum feature sizes of $t_1$ and $t_2$ (40 nm). This can be mitigated by introducing smaller minimum feature sizes to $t_1$ and $t_2$, which leads to relax a refractive

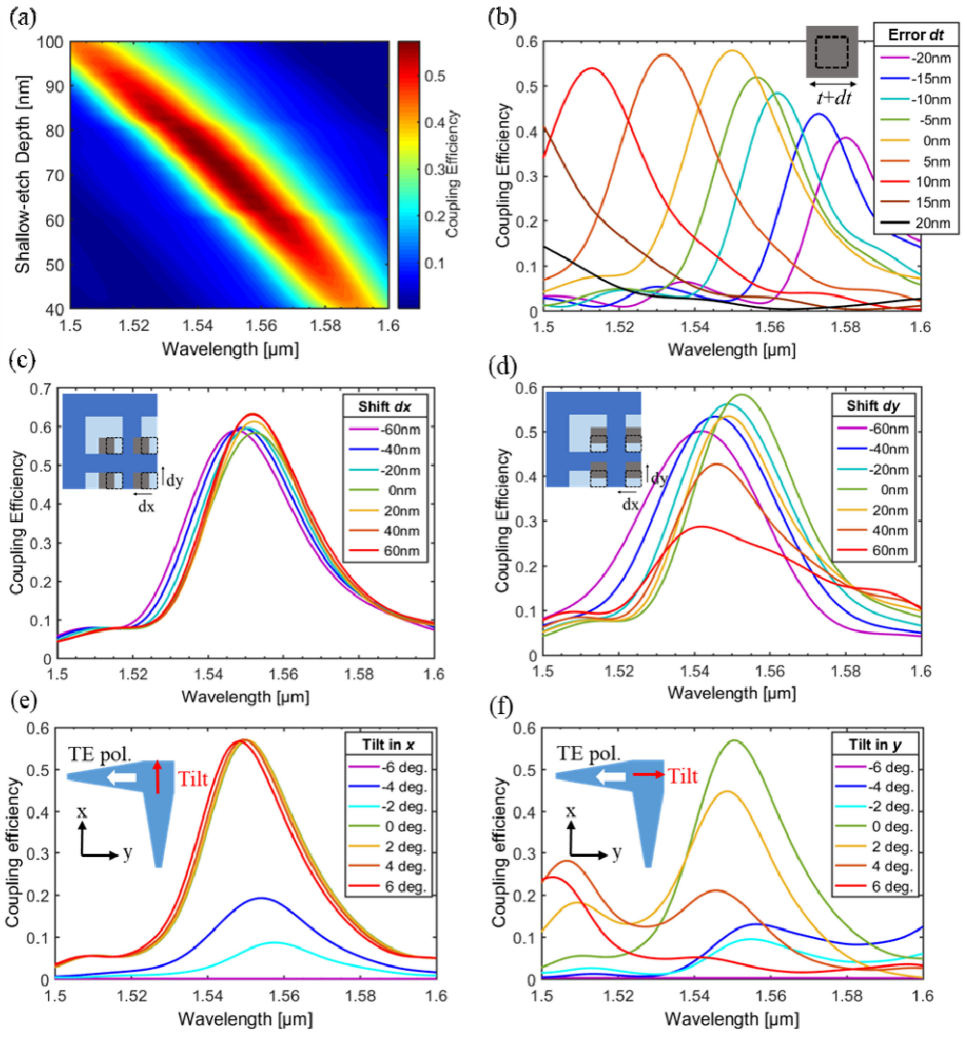


Fig. 4. Fabrication tolerance of the 2-D grating couplers. Dependencies of the coupling efficiency on (a) the shallow-etch depth, (b) the fully etched feature width, (c–d) misalignments between fully and shallow etched features in x- and y-direction and (e–f) tilt angles of the fiber coupling, respectively. In plots (e) and (f), the fiber is tilted along *x* and *y* axes from the chip surface normal. Here, all the simulations have been performed for with an x-polarization excitation. For a y-polarization, the x and y axes need to be inverted within the plots (c f).

index discontinuity at the interface between the waveguide and the grating and to decrease the field intensity diffracted from the first period of gratings.

Next, we investigated the fabrication tolerance of various parameters such as the depth tolerance of shallow-etched features, and the alignment and width tolerance of the fully-etched features. Fig. 4(a) shows the calculated results of the coupling efficiency against changes of the shallow-etch depth. A coupling efficiency of $>$50% can be maintained for deviations up to $\pm$5 nm from the ideal 70 nm for a wavelength of 1550 nm. Fig. 4(b) shows the tolerance towards width variations *dt* of $t_1$ and $t_2$. It can be seen that the 2-D grating coupler is more tolerant towards an increase of the fully etched feature width in terms of coupling efficiency. Figs. 4(c) and 4(d) shows the coupling efficiency against a misalignment *dx* or *dy* in *x*- or *y*-direction of the fully etched features with respect to the shallow etched structures, respectively. In the simulation, the polarization of interest is an x-polarization. In Figs. 4(c) and 4(d), we observe a blue shift of the peak wavelength for misalignment in the x- as well as y-directions. This is because the effective refractive index of the grating reduces

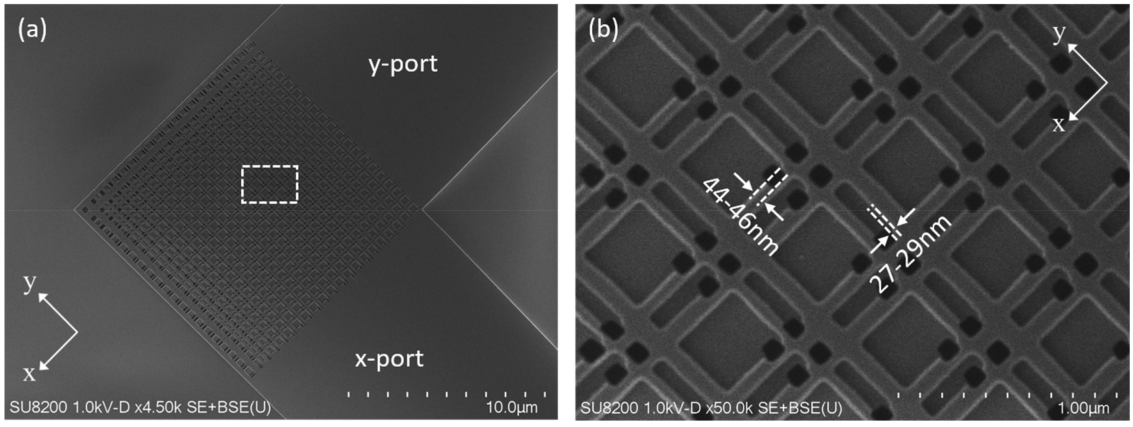


Fig. 5. Scanning electron microscopic images of fabricated 2-dimensional grating coupler on a standard silicon-on-insulator chip. (a) Top-view picture of the 2-dimenstional grating. (b) Magnified view of the area that is highlighted in (a).

as the fully etched structures affect the un-etched silicon parts when they are misaligned. The shift in x-direction slightly increases the coupling efficiency, whereas a shift in y-direction has a more pronounced influence on the efficiency and the peak positions. Although it seems that one can improve the coupling efficiency by shifting the holes along the x-direction, this leads to a reduced coupling efficiency of the other polarization port. Moreover, as shown in Fig. 4(d), a shift in the negative y-direction has a smaller impact on the coupling efficiency compared to a shift in the positive y-direction. In Figs. 4(e) and 4(f), we have simulated the coupling efficiency dependence on the fiber tilt. The fiber is tilted along *x* or *y* coordinate axes with some degrees from the chip surface normal whilst the waveguides are fixed. The 2-D grating coupler is more tolerant to the fiber tilt in positive directions than that in negative directions as shown in these figures. In a certain case where the fiber is tilted along the input polarization axis in positive directions (which is the positive direction tilts in Fig. (e)), a variation of the coupling spectrum is small.

## 3. Fabrication and Characterization

We fabricated the 2D grating couplers on a commercially available SOI wafer with a 220 nm-thick silicon layer and 3.0 $\mu$m-thick BOX layer. In a first step the 70 nm-deep shallow etch features were defined by electron-beam (EB) lithography (Vistec EBPG5200) using a positive tone resist, followed by an inductively coupled plasma dry-etching process with HBr-ions (Oxford Plasmofab System 100). Next, the waveguides and fully etched holes were defined with a negative-tone resist and dry-etching process similar to the partially etched one. Finally, a 1.5 $\mu$m-thick silicon dioxide ($SiO_2$) layer as a top-cladding was deposited using a plasma-enhanced chemical vapor deposition (PECVD). Fig. 5 shows scanning electron microscope (SEM) images of the fabricated device before depositing the cladding $SiO_2$. Fig. 5(a) shows a picture of the entire 2-D grating area where the 2-D grating coupler is connected to x- and y-ports via tapered waveguides. The fabricated devices consist of a 2-D grating coupler with two 300 $\mu$m-long tapered waveguides, each connected to 1-D grating couplers from [4] used as outputs. The 2-D grating couplers are connected to the 1-D grating couplers via 450 nm-wide waveguides.

We performed insertion loss measurements to characterize the fabricated 2-D grating couplers. From the measurement, we obtained coupling efficiencies of $-2.6$ dB at 1544 nm wavelength for the x-port and $-3.4$ dB at 1536 nm wavelength for the y-port. The 3 dB bandwidth was 36 nm and 27 nm for x- and y-ports, respectively. We also measured crosstalks of $-16.2$ dB to the x-port from the y-polarization input and $-20.8$ dB to the y-port from the x-polarization input at the maximum. Fig. 6 summarizes simulated and measured coupling efficiencies and crosstalks of the 2-D grating

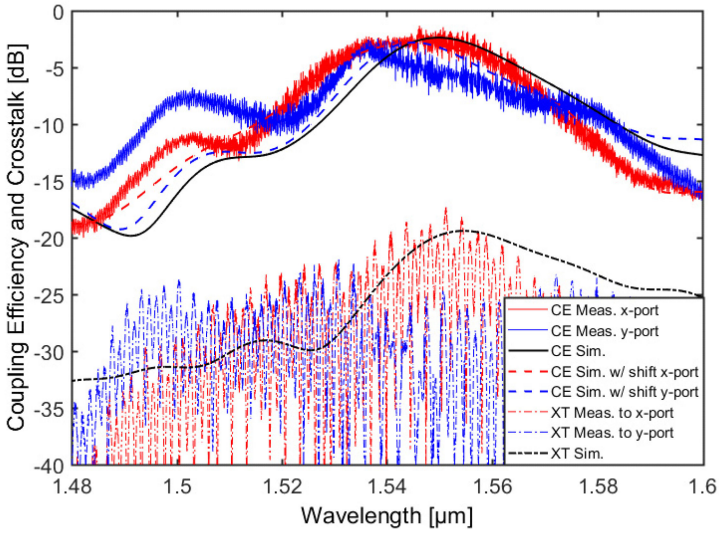


Fig. 6. Measured and simulated coupling efficiencies and crosstalk of the 2-D grating coupler.

couplers. The insertion loss was measured using a tunable laser source and a power meter for each polarization port separately. Either x- or y-polarized $LP_{01}$ modes were launched into the 2-D grating couplers using a vertically aligned SMF and the outputs from the 1-D grating couplers were collected using another SMF. Here, we applied an index matching oil in between the fiber and the cladding surface, so that we can suppress the reflections and refractions at those surfaces. The input polarization state was aligned using a polarization controller so that the insertion loss of the port of interest is minimized. Then we also measured the insertion loss of the opposite polarization port while maintaining the input polarization state in order to characterize the crosstalk of the 2-D grating coupler. We isolated the coupling efficiency and the crosstalk of the 2D-grating coupler from the measured insertion losses by subtracting the propagation loss in the Si waveguide (0.43 dB/mm), the back-to-back loss and the input 1-D grating coupler from the loss spectrum, which have been characterized separately. Additionally, we have estimated reflectivities of the back-reflection of the 2D grating coupler by using Fabry-Perot ripples as observed from measured spectra. The reflectivities are approximately 11%, 1% and 15% at 1520 nm, 1540 nm and 1560 nm wavelengths, respectively.

In Fig. 6, we have plotted simulated and measured coupling efficiencies (CEs) and crosstalks (XTs) for both the ideal structure and the fabricated coupler with the respective deviations of $-45$ and 28 nm in x- and y-directions, respectively, from the proper alignment (see experimental description above). These deviations actually lead to a modified passband, see Fig. 6. Particularly, the y-port will suffer from a blue-shift of the center passband and a reduced bandwidth as can be seen from the solid blue plot in Fig. 6. This narrowing of the passband is also found in the experiment (see blue dashed curve). For the y-polarization port, tendencies of the coupling characteristic variations are consistent between measured and simulated values in terms of a blue shift of the peak wavelength and a narrowing of the bandwidth. This issue can be solved by a better control over the fabrication.

We have further characterized the performance of the 2-D grating coupler by measuring the polarization dependent loss (PDL). That is the ratio between maximum ($T_{\max}$) and minimum ($T_{\min}$) transmissions while the input polarization is changed over all possible states [15],

$$PDL\ (\text{dB}) = \left| 10 \log_{10} \left( \frac{T_{\max}}{T_{\min}} \right) \right| .$$

We launched the $LP_{01}$ mode into the same 2-D grating coupler as discussed above with random polarization states and measured a sum of transmissions from two output ports. In Fig. 7, we

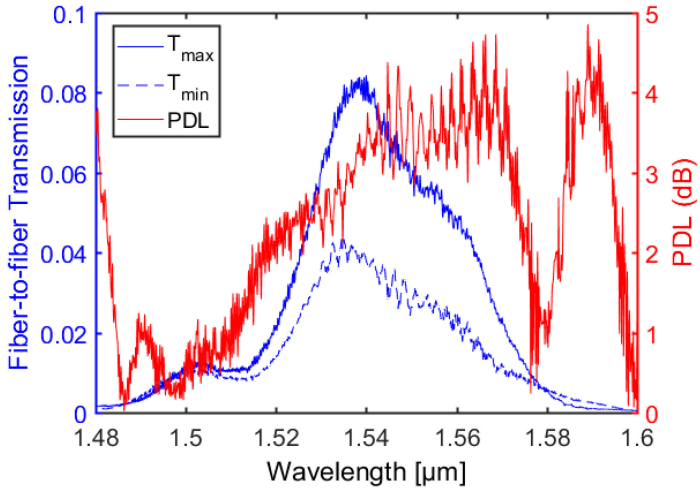


Fig. 7. Measured polarization dependent loss (PDL) the 2-D grating coupler.

show the measured fiber-to-fiber transmissions and PDL of the 2-D grating coupler. Due to the vertical coupling angle [34], there is no peak-wavelength shift between maximum and minimum transmission spectra. We, however, still observe a PDL of approximately 3 dB around the peak-wavelength of 1540 nm. This mainly comes from the difference of coupling spectra between x- and y-port due to the asymmetry of the fabricated structure.

## 4. Conclusions

We have demonstrated a highly efficient 2-D grating coupler which couples both x- and y-polarized $LP_{01}$ modes into TE silicon waveguide modes with perfectly vertical fiber angles. We fabricated the couplers on a standard SOI wafer, using a simple 2-step etching process that is CMOS compatible. The experimentally measured coupling efficiencies were $-2.6$ dB and $-3.4$ dB for $LP_{01}{}^{x}$ and $LP_{01}{}^{y}$ modes, respectively. The perfectly vertical coupling scheme allows our grating coupler to achieve a high integration density for use in reduced diameter fiber arrays and multi-core fibers (MCF).

## References

[1] R. Marchetti *et al.*, "High-efficiency grating-couplers: Demonstration of a new design strategy," *Sci. Rep.*, vol. 7, no. 1, pp. 1–8, 2017.
[2] D. Benedikovic *et al.*, "Subwavelength index engineered surface grating coupler with sub-decibel efficiency for 220-nm silicon-on-insulator waveguides," *Opt. Exp.*, vol. 23, no. 17, pp. 22628–22635, 2015.
[3] J. Notaros *et al.*, "Ultra-efficient CMOS fiber-to-chip grating couplers," in *Proc. Opt. Fiber Commun. Conf.*, Anaheim, CA, USA, 2016.
[4] T. Watanabe, M. Ayata, U. Koch, Y. Fedoryshyn, and J. Leuthold, "Perpendicular grating coupler based on a blazed antiback-reflection structure," *J. Lightw. Technol.*, vol. 35, no. 21, pp. 4663–4669, Nov. 2017.
[5] A. Bozzola, L. Carroll, D. Gerace, I. Cristiani, and L. C. Andreani, "Optimising apodized grating couplers in a pure SOI platform to $-0.5$ dB coupling efficiency," *Opt. Exp.*, vol. 23, no. 12, pp. 16289–16304, 2015.
[6] A. Michaels and E. Yablonovitch, "Inverse design of near unity efficiency perfectly vertical grating couplers," *Opt. Exp.*, vol. 26, no. 4, pp. 4766–4779, 2018.
[7] D. Taillaert, P. Bienstman, and R. Baets, "Compact efficient broadband grating coupler for silicon-on-insulator waveguides," *Opt. Lett.*, vol. 29, no. 23, pp. 2749–2751, 2004.
[8] G. Roelkens, D. Van Thourhout, and R. Baets, "High efficiency silicon-on-insulator grating coupler based on a poly-Silicon overlay," *Opt. Exp.*, vol. 14, no. 24, pp. 11622–11630, 2006.
[9] X. Chen, C. Li, C. K. Y. Fung, S. M. G. Lo, and H. K. Tsang, "Apodized waveguide grating couplers for efficient coupling to optical fibers," *IEEE Photon. Technol. Lett.*, vol. 22, no. 15, pp. 1156–1158, Aug. 2010.
[10] D. Benedikovic *et al.*, "High-directionality fiber-chip grating coupler with interleaved trenches and subwavelength index-matching structure," *Opt. Lett.*, vol. 40, no. 18, pp. 4190–4193, 2015.

[11] A. Melikyan, T.-C. Hu, K. Kim, Y. Baeyens, M. Earnshaw, and P. Dong, "Efficient optical I/O in standard SiPh process," in *Proc. Opt. Fiber Commun. Conf.*, San Diego, CA, USA, 2019, Paper Tu2J.5.
[12] D. Taillaert, C. Harold, P. I. Borel, L. H. Frandsen, R. M. D. L. Rue, and R. Baets, "A compact two-dimensional grating coupler used as a polarization splitter," *IEEE Photon. Technol. Lett.*, vol. 15, no. 9, pp. 1249–1251, Sep. 2003.
[13] M. F. Rosa, P. d. I. T. Castro, N. Hoppe, L. Rathgeber, W. Vogel, and M. Berroth, "Novel design of two-dimensional grating couplers with backside metal mirror in 250 nm silicon-on-insulator," in *Proc. Int. Conf. Numer. Simul. Optoelectron. Devices*, 2017, pp. 81–82.
[14] Y. Luo *et al.*, "Low-loss two-dimensional silicon photonic grating coupler with a backside metal mirror," *Opt. Lett.*, vol. 43, no. 3, pp. 474–477, 2018.
[15] F. V. Laere *et al.*, "Focusing polarization diversity grating couplers in silicon-on-insulator," *J. Lightw. Technol.*, vol. 27, no. 5, pp. 612–618, Mar. 2009.
[16] L. Verslegers *et al.*, "Design of low-loss polarization splitting grating couplers," in *Advanced Photonics for Communications*. San Diego, CA, USA: Optical Society of America, 2014, Paper JT4A.2.
[17] C. Lacava *et al.*, "Design and characterization of low-loss 2D grating couplers for silicon photonics integrated circuits," *Proc. SPIE*, vol. 9752, pp. 97520V, 2016.
[18] W. Wu, T. Lin, T. Chu, and H. Zhang, "CMOS-compatible high efficiency polarization splitting grating coupler near 1310nm," in *Proc. Asia Commun. Photon. Conf.*, Wuhan, China, 2016, Paper AS2F.4.
[19] C. R. Doerr and T. F. Taunay, "Silicon photonics core-, wavelength-, and polarization-diversity receiver," *IEEE Photon. Technol. Lett.*, vol. 23, no. 9, pp. 597–599, May 2011.
[20] V. I. Kopp *et al.*, "Two-dimensional, 37-channel, high-bandwidth, ultra-dense silicon photonics optical interface," *J. Lightw. Technol.*, vol. 33, no. 3, pp. 653–656, Feb. 2015.
[21] Y. Ding, F. Ye, C. Peucheret, H. Ou, Y. Miyamoto, and T. Morioka, "On-chip grating coupler array on the SOI platform for fan-in/fan-out of MCFs with low insertion loss and crosstalk," *Opt. Exp.*, vol. 23, no. 3, pp. 3292–3298, 2015.
[22] X. Chen, C. Li, and H. K. Tsang, "Two dimensional silicon waveguide chirped grating couplers for vertical optical fibers," *Opt. Commun.*, vol. 283, no. 10, pp. 2146–2149, 2010.
[23] C. R. Doerr *et al.*, "Monolithic polarization and phase diversity coherent receiver in silicon," *J. Lightw. Technol.*, vol. 28, no. 4, pp. 520–525, Feb. 2010.
[24] J. Zou *et al.*, "An SOI based polarization insensitive filter for all-optical clock recovery," *Opt. Exp.*, vol. 22, no. 6, pp. 6647–6652, 2014.
[25] Z. Jinghui, Y. Yu, Y. Mengyuan, L. Lei, D. Shupeng, and Z. Xinliang, "A four-port polarization diversity coupler for vertical fiber-chip coupling," in *Proc. Opt. Fiber Commun. Conf. Exhib.*, 2015, pp. 1–3.
[26] Y. Wang *et al.*, "Focusing sub-wavelength grating couplers with low back reflections for rapid prototyping of silicon photonic circuits," *Opt. Exp.*, vol. 22, no. 17, pp. 20652–20662, 2014.
[27] W. S. Zaoui *et al.*, "Bridging the gap between optical fibers and silicon photonic integrated circuits," *Opt. Exp.*, vol. 22, no. 2, pp. 1277–1286, 2014.
[28] Y. Ding, C. Peucheret, H. Ou, and K. Yvind, "Fully etched apodized grating coupler on the SOI platform with -0.58dB coupling efficiency," *Opt. Lett.*, vol. 39, no. 18, pp. 5348–5350, 2014.
[29] F. V. Laere *et al.*, "Compact focusing grating couplers for silicon-on-insulator integrated circuits," *IEEE Photon. Technol. Lett.*, vol. 19, no. 23, pp. 1919–1921, Dec. 2007.
[30] J. Kang *et al.*, "Amorphous-silicon inter-layer grating couplers with metal mirrors toward 3-D interconnection," *IEEE J. Sel. Topics Quantum Electron.*, vol. 20, no. 4, pp. 317–322, Jul./Aug. 2014.
[31] D. Vermeulen *et al.*, "High-efficiency fiber-to-chip grating couplers realized using an advanced CMOS-compatible Silicon-On-Insulator platform," *Opt. Exp.*, vol. 18, no. 17, pp. 18278–18283, 2010.
[32] J. Robinson and Y. Rahmat-Samii, "Particle swarm optimization in electromagnetics," *IEEE Trans. Antennas Propag.*, vol. 52, no. 2, pp. 397–407, Feb. 2004.
[33] A. Dorodnyy, V. Shklover, L. Braginsky, C. Hafner, and J. Leuthold, "High-efficiency spectrum splitting for solar photovoltaics," *Solar Energy Mater. Solar Cells*, vol. 136, pp. 120–126, 2015.
[34] F. V. Laere *et al.*, "Nanophotonic polarization diversity demultiplexer chip," *J. Lightw. Technol.*, vol. 27, no. 4, pp. 417–425, Feb. 2009.